Available online at www.sciencedirect.com
SCIENCE DIRECT®
Optics Communications 246 (2005) 313–321
OPTICS COMMUNICATIONS
www.elsevier.com/locate/optcom

Axial resolution in two-color excitation fluorescence microscopy by phase-only binary apodization

M.T. Caballero [a,*], P. Andrés [b], A. Pons [b], J. Lancis [c], M. Martínez-Corral [b]

[a] Departamento de Óptica, Universidad de Alicante, Campus San Vicente del Raspeig, P.O. Box 99, E03080 Alicante, Spain
[b] Departamento de Óptica, Universidad de Valencia, E46100 Burjassot, Spain
[c] Departamento de Ciencias Experimentales, Universitat Jaume I, E12080 Castellón, Spain

Received 30 July 2004; received in revised form 13 October 2004; accepted 8 November 2004

Abstract

We study the effect of a kind of binary phase-only filters, the Toraldo filters, in two-color excitation fluorescence microscopy. We show that by simple insertion of a properly designed Toraldo filter in one of the illumination arms the axial resolution of the system is significantly improved. Specifically, the main peak of the point spread function is narrowed by 22% along the axial direction.

PACS: 42.79.Ci; 42.25.Fx; 42.30.Va
Keywords: Superresolution; Toraldo filters; Two-color excitation microscopy

1. Introduction

In fluorescence microscopy, resolving power depends on the extent of the point-spread function (PSF), which is a mathematical description of the intensity distribution in the focal region of an objective lens. The smaller the extent of the PSF, the better the images of individual points, and therefore, the better resolution is achieved. However, when an optical fluorescence microscope is used, the images of parts at a certain depth in the sample contain blurred information about the entire one. The use of confocal scanning technique [1] allows the improvement of the contrast of images because of the pinholed detection. However, when fluorescence excitation is produced by the incident beam, photobleaching is generated not only at the scanned region, but on the entire sample. This is an important drawback because some parts of the fluorescent sample are bleached before than imaged.

* Corresponding author. Tel.: +34 965903400 3390; fax: +34 965903464.
E-mail address: mt.caballero@ua.es (M.T. Caballero).

0030-4018/$ - see front matter © 2004 Elsevier B.V. All rights reserved.
doi:10.1016/j.optcom.2004.11.035

Because of research in cellular structures, new excitation processes have been proposed in recent years [2–4]. In case of two-photon excitation (2PE), the fluorescence signal is proportional to the square of the excitation intensity and therefore is strongly confined into a small region around the focal point of the objective lens. This process inherently possesses high optical-sectioning capacity even with a large area photodetector. The excitation wavelength is $\lambda_{2p} = 2\lambda_e$,$\lambda_e$ being the single-photon excitation wavelength. This longer and near-infrared wavelength provides the excitation beam with a deeper penetration capacity. A thorough review of the advantages of 2PE scanning microscopes over 1PE ones is done in [5].

On the other hand, since two statistically independent events have to occur in 2PE, the fluorescence probability is proportional to the square of the excitation intensity. As a result of that the PSF of 2PE is much wider in the axial direction than in the lateral one. This implies despite of its high optical sectioning capacity, 2PE microscopes still exhibit an axial resolution that is much poorer than the lateral resolution. Some techniques to improve axial and transverse resolution in two-photon or multiphoton processes have been studied [6,7].

In recent years, two-color excitation (2CE) fluorescence microscopy has been proposed [8,9]. In this case, two excitation photons of different wavelengths λ_1 and λ_2 are used to excite the specimen. The wavelengths verify the relation $2/\lambda_{2p} = 1/\lambda_1 + 1/\lambda_2$. The 2PE microscopy is only a special case of 2CE microscopy where $\lambda_1 = \lambda_2 = \lambda_{2p}$. In a 2CE microscope the fluorescence intensity is generated only in regions where the excitation beams overlap with each other in both space and time. One advantage of 2CE is its capacity for observation of microscopic objects through highly scattering media [10–12]. In 2CE imaging, scattering decreases the in-focus fluorescence but hardly increases the undesirable fluorescence background unlike in the 2PE case. In spite of difficulty to realize the experimental setup, the linear dependence of the 2CE point spread function with the product of the excitation intensities has been verified [13,14].

The 2CE process has been studied [15] and applied to different optical-sectioning architectures [16–18]. Due to the difference in wavelength between the two illumination beams, a more efficient process than the 2PE can be achieved. This fact allows the use of superresolving elements to improve the axial resolution. Here, we propose the use of phase-only Toraldo filters in a 2CE system to produce a compression of the axial PSF and consequently, an improvement of the optical-sectioning power.

2. Theory

We start by considering a 2CE fluorescence scanning microscope, schematically shown in Fig. 1. The PSF of such a system is given by

$$\mathrm{PSF}_{2\mathrm{CE}}(r,z;\lambda_1,\lambda_2) = |h_1(r,z;\lambda_1)|^2 \cdot |h_2(r,z;\lambda_2)|^2, \tag{1}$$

where h_1 and h_2 represent the amplitude PSFs of the illumination beams. The $\mathrm{PSF}_{2\mathrm{CE}}$ is obtained as a product of two independent PSFs, which are scaled proportionally to λ_1 and λ_2. Since this kind of microscope always operates with high numerical-aperture objectives, the accurate calculation of the PSFs must be done according to the vectorial Debye theory [19]. To such end, the polarization state of illumination light and the vectorial condition of the electric field at an observation point near the focal volume must be taken into account. If we consider a monochromatic, linearly polarized plane wavefront that impinges on the aberration-free high-aperture objective, then the electric field at an observation point within the focal volume is given by a three-dimensional function that can be expressed as [20],

$$\mathbf{E}(r,z,\psi) = \frac{\pi \mathrm{i}}{\lambda}\{[I_0 + \cos(2\psi)I_2]\mathbf{i} + \sin(2\psi)I_2\mathbf{j} + 2\mathrm{i}\cos\psi I_1\mathbf{k}\}, \tag{2}$$

where ψ is the angle between the polarization direction of the incident field (assumed without any loss of generality to be in the x-direction) and the meridian plane under study. I_0, I_1 and I_2 are integrals over the aperture angle θ:

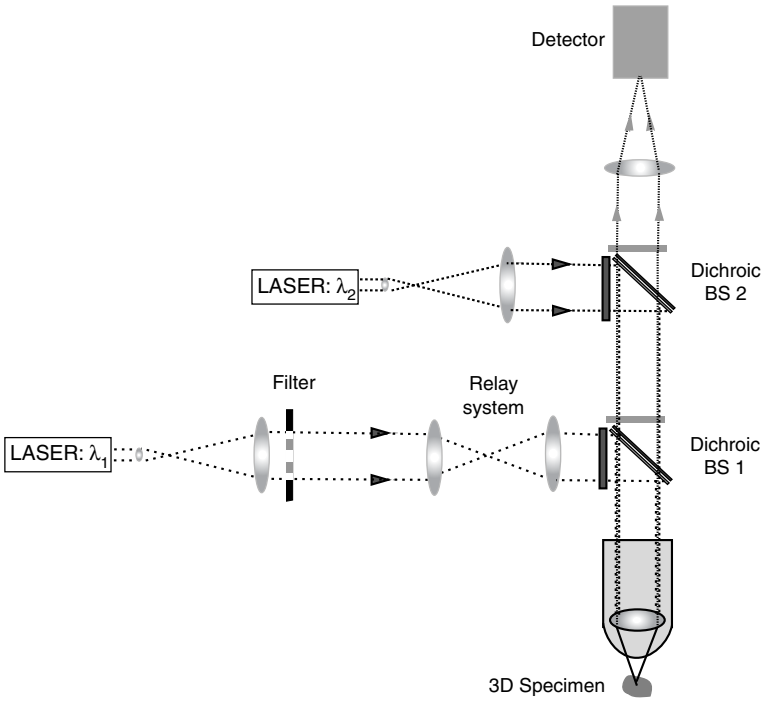

Fig. 1. Experimental setup of a 2CE fluorescence scanning microscope.

$$I_0 = \int_0^{\alpha} P(\theta)\sin\theta(1+\cos\theta)J_0(kr\sin\theta) \times \exp(-\mathrm{i}kz\cos\theta)\mathrm{d}\theta, \tag{3}$$

$$I_1 = \int_0^{\alpha} P(\theta)\sin^2\theta J_1(kr\sin\theta) \times \exp(-\mathrm{i}kz\cos\theta)\mathrm{d}\theta, \tag{4}$$

$$I_2 = \int_0^{\alpha} P(\theta)\sin\theta(1-\cos\theta)J_2(kr\sin\theta) \times \exp(-\mathrm{i}kz\cos\theta)\mathrm{d}\theta, \tag{5}$$

where r and z are the cylindrical coordinates as measured from the focal point, $P(\theta)$ accounts for the amplitude transmittance at the pupil of the lens and α is the maximum value of the aperture angle θ.

Next we focus our attention in the axial response. Then we set $r = 0$ in previous equations. Note that since first and second order Bessel functions are null in the origin, the axial amplitude is polarized in the same direction as the incident beam, that is,

$$\mathbf{E}_0(z) = \mathbf{E}(r=0,z) = \mathbf{i}\frac{\pi\mathrm{i}}{\lambda}\int_0^{\alpha} P(\theta)(1+\cos\theta) \times \exp\left(-\mathrm{i}2\pi n\frac{\cos\theta}{\lambda}z\right)\sin\theta\,\mathrm{d}\theta. \tag{6}$$

The axial behaviour can be analysed in simpler way if we perform the nonlinear mapping,

$$\zeta = \frac{\cos\theta-\cos\alpha}{1-\cos\alpha} - 0.5, \qquad (\zeta) = (1+\cos\theta)P(\theta). \tag{7}$$

Then Eq. (6) can be rewritten, aside from a multiplying linear phase factor, as

$$h(0,z_N) = E_0(z_N) = (1-\cos\alpha) \times \int_{-\infty}^{\infty} q(\zeta)\exp(-\mathrm{i}2\pi z_N\zeta)\mathrm{d}\zeta, \tag{8}$$

where the axial position is expressed in terms of the normalized non-dimensional variable,

$$z_N = \frac{n}{\lambda}(1-\cos\alpha)z. \tag{9}$$

Since the field $\mathbf{E}_0(z)$ is linearly polarized along the x direction, we have omitted the explicit reference to its vectorial character in Eq. (8). Therefore, the axial PSF is obtained from a simple one-dimensional Fourier transformation of $q(\zeta)$.

The objective of this research is the improvement of axial resolution, and consequently the three-dimensional (3D) one, by Toraldo filters. We propose to insert such type of phase filters in the illumination beam of smaller wavelength. This allows to increment the PSFs scale mismatch and therefore to produce a great compression of the central lobe of the overall 2CE PSF.

3. Filters synthesis

To start with the process of filters design, we consider the properties of phase-only filters designed according Toraldo concept [21]. Toraldo di Francia showed that the radii of the zero-intensity rings in the focal plane of a paraxially focusing system can be selected at will by using a pupil filter subdivided into concentric zones with constant transmittance. In the original Toraldo algorithm the amplitude transmittance of the filter, is subdivided into m concentric annular zones to control the radii of $m-1$ rings of zero intensity. An exhaustive analysis of annular phase only filters with desired focal characteristics has been made in [22,23].

Like in the original paraxial procedure, here we have a Fourier transform relation between the nonlinearly mapped transmittance of the filter, and the axial PSF evaluated according the vectorial non-paraxial theory. Therefore, Toraldo concept can be applied to this new situation [24]. Then, by dividing function $q(\zeta)$ into $2m-1$ subintervals of constant transmittance, one can control the positions of $m-1$ axial zeros, namely,

$$q(\zeta) = k_1 \operatorname{rect}\left(\frac{\zeta}{\Delta_1}\right) + \sum_{i=1}^{m-1} k_{i+1}\left[\operatorname{rect}\left(\frac{\zeta}{\Delta_{i+1}}\right) - \operatorname{rect}\left(\frac{\zeta}{\Delta_i}\right)\right], \quad (10)$$

where $\Delta_m = 1$, $\Delta_i > \Delta_{i-1}$, $m \geqslant 2$, and k_i is the transmittance of the ith zone. The axial PSF is calculated by Eq. (9),

$$h(0,z_N) = \sum_{i=1}^{m} k_i[\Delta_i \operatorname{sinc}(\Delta_i z_N) - \Delta_{i-1}\operatorname{sinc}(\Delta_{i-1} z_N)]. \quad (11)$$

In the particular case of $m = 2$,

$$h(0,z_N) = (k_1 - k_2)\Delta \operatorname{sinc}(\Delta z_N) + k_2 \operatorname{sinc}(\Delta z_N), \quad (12)$$

with $\Delta = \Delta_1$.

We apply now the design constraint by selecting the zero in the axial point z_1,

$$(k_1 - k_2)\Delta \operatorname{sinc}(\Delta z_1) + k_2 \operatorname{sinc}(\Delta z_1) = 0. \quad (13)$$

To maximize the filter throughput, the two zones should have opposite phases,

$$k_2 = -k_1 = 1. \quad (14)$$

Then, we obtain the transcendental equation,

$$\Delta = \frac{\operatorname{sinc}(z_1)}{2\operatorname{sinc}(\Delta z_1)}, \quad (15)$$

whose solution determines the width of the zones. A similar deduction could be made to select a filter with a bigger number of zones.

4. Numerical results

To show the validity of our approach, we have chosen a 2CE system where $\lambda_1/\lambda_2 = 0.9$ (in other words $\lambda_1 = 0.95\lambda_{2p}$ and $\lambda_2 = 1.06\lambda_{2p}$). To improve the axial resolution in 2CE fluorescence microscopy, we have designed a seven-zone Toraldo filter whose shape and axial response are shown in Fig. 2. In the design procedure, we fixed the first zero in $z_N = 0.6$, what entails a reduction of central lobe width by 40%. The second and third ones were fixed at $z_N = 1.6$ and $z_N = 2.7$, respectively. Therefore, the parameters of the filter are $\Delta_1 = 0.11$, $\Delta_2 = 0.39$ and $\Delta_3 = 0.64$. In Fig. 3 we show the axial PSFs corresponding to the illuminating arms. Because of the wavelengths mismatch, the first zero of axial PSF in the second arm is not at $z_N = 1.0$ but at $z_N = 1.1$.

Note that the use of Toraldo filters inherently produces an important increase of sidelobes height. Such sidelobes would be very detrimental

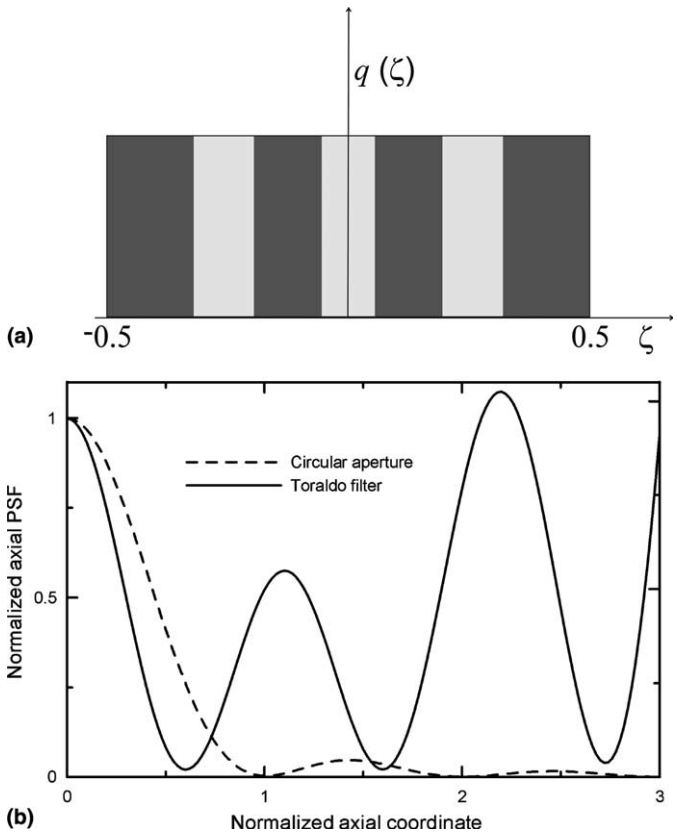

Fig. 2. (a) Seven-zone Toraldo filter; (b) normalized axial PSF of the Toraldo filter (solid line) compared to the one of the circular aperture (dashed line).

in other scanning fluorescence techniques (like 1PE confocal microscopy or 2PE scanning microscopy) since they produce an undesirable photobleaching in the entire sample when any single plane is imaged. However, in 2CE microscopy the fluorescence intensity is generated only in regions where the excitation beams overlap with each other in both space and time. Note then from Fig. 3 that the maxima of PSF_1 coincide with the minima of PSF_2. Therefore, in the resulting overall PSF the main-peak has been importantly narrowed, and the axial sidelobes have been almost annihilated. Besides, the use of the proposed filters hardly affects the lateral resolution. To show that, the 3D overall PSF is depicted in Fig. 4 where we compare a 2CE system with the Toraldo filter inserted in arm-1, with a reference 2CE experiment in which no filter is inserted. Note that the sidelobes height is always below 3%.

To show the robustness of our method, next we perform numerical experiments with two systems with different λ_1/λ_2 ratio. We have chosen two configurations suggested in other publications: (a) $\lambda_{2p} = 800$ nm, $\lambda_1 = 785.3$ nm and $\lambda_2 = 815.3$ nm [17]; and (b) $\lambda_{2p} = 700$ nm, $\lambda_1 = 656$ nm and $\lambda_2 = 750$ nm [15]. For the calculations we considered selected an objective of NA = 1.40 (oil). The wavelengths ratio is 0.96 in the first case and 0.87 in the second one, bigger and smaller, respectively, than our previous example. In Fig. 5 we compare the axial intensity in 2CE fluorescence microscopy with and without the Toraldo filter. Also, we show the axial intensity in 2PE with the Toraldo filter. Note that the use of Toraldo filters in 2PE is not useful because they produce very

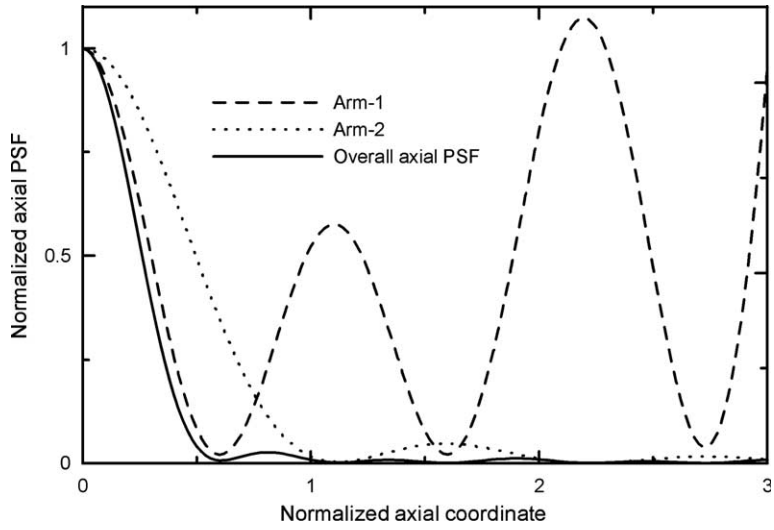

Fig. 3. Normalized axial PSFs of the system. Dashed-line curve corresponds to the PSF of arm-1 (Toraldo filter), dotted-line curve to arm-2 (circular aperture), and solid-line curve to the overall axial PSF.

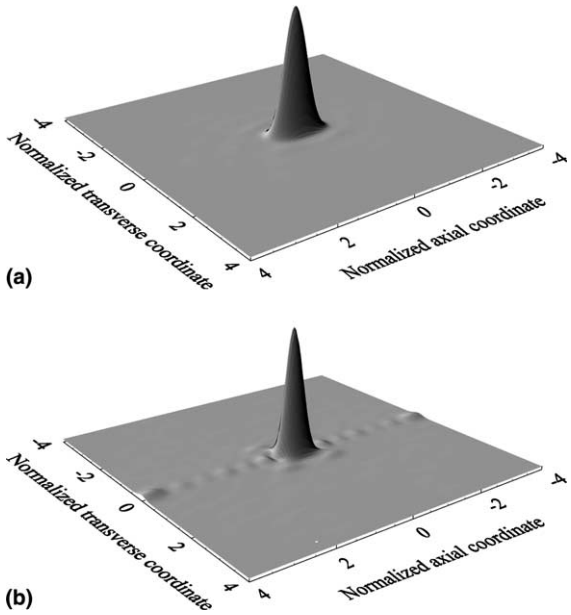

Fig. 4. (a) 3D PSF of a 2CE microscope with the circle as the pupil stop in both arms; (b) same, but after inserting a seven-zone Toraldo filter in arm-1.

high sidelobes which destroy the contrast of the 3D images and produce important photobleaching. However, Toraldo filters are very useful in 2CE due to the annihilation of the sidelobes. In our examples the main peak is narrowed by 21.8% and 23.1%, respectively. Concerning the sidelobes, their maximum height is 1.75% and 3.1%, respectively.

5. Application to other scanning geometries

Next we wonder if Toraldo filters can be efficiently used to improve the performance of other 2CE architectures. First we consider the case of the so-called θ-microscopy technique [25,26]. In this technique, the optical axis of the illumination arm-2 is set at angle θ ($0 < \theta\pi/2$) with respect to the axis of arm-1 [10–12]. Due to the ellipsoidal shape of the PSFs, the axial extension of the PSF-1 is strongly reduced after multiplication by the lateral section of PSF-2. Calculations, not shown, demonstrate that the above-proposed Toraldo filters are not useful in this kind of geometry. This is because the axial width of the overall PSF is determined by the lateral width of PSF-2, which is about 3 times narrower the axial width of PSF-1. Therefore it is nonsense to use a filter to narrow PSF-1 in the axial direction by, for example, 40%. This narrowness hardly produce any effect on the axial width of the overall PSF. So, in

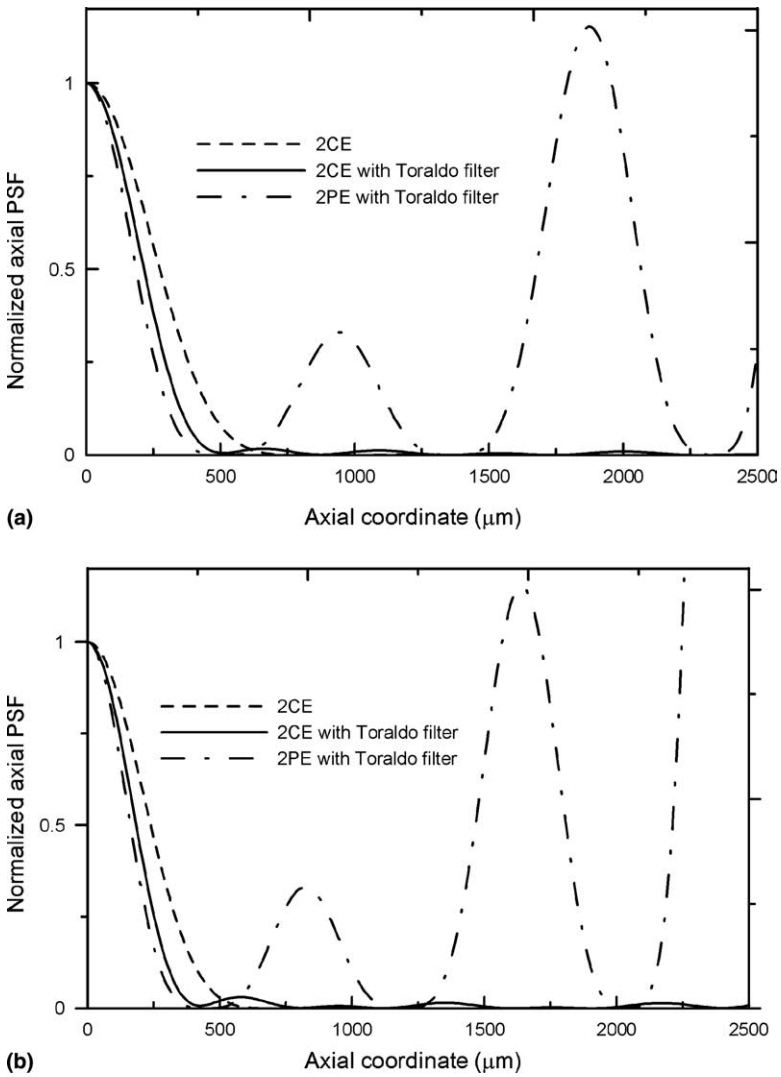

Fig. 5. Normalized axial PSF of: 2CE microscopy system with two circular apertures (dashed line); idem but with the Toraldo filter in the arm-1 (solid line) and normalized axial PSF of the 2PE microscope with the Toraldo filter (dot dashed line). (a) First configuration: $\lambda_{2p} = 800$ nm, $\lambda_1 = 785.3$ nm and $\lambda_2 = 815.3$ nm. (b) Second configuration: $\lambda_{2p} = 700$ nm, $\lambda_1 = 656$ nm and $\lambda_2 = 750$ nm.

this case the Toraldo filters would reduce the light efficiency of the microscope, and would not improve its optical sectioning capacity.

We have also considered the 4Pi architecture [27]. In this case, two opposite beams with λ_1 and λ_2, respectively, interfere constructively and illuminate the sample. The resultant PSF is sharper than the one in conventional microscopy, but with some important sidelobes that can lead to ambiguity in the image [18]. The effect of Toraldo filter in 4Pi microscopy consists of the attenuation of these sidelobes height, as we show in Fig. 6. Using the 2CE configuration suggested in [17] and a properly designed seven-zone Toraldo filter, the height of sidelobes can be reduced up to nearly 70%. We also include the results

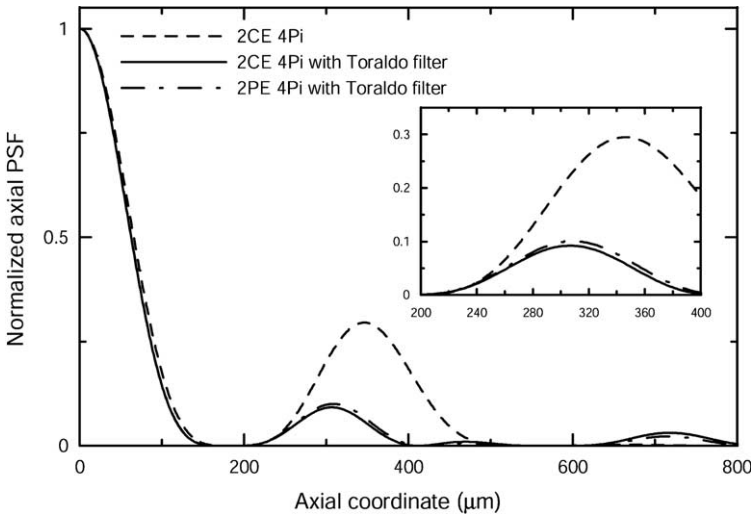

Fig. 6. Normalized axial PSF of: 2CE 4Pi microscopy system with two circular apertures (dashed line); idem but with the Toraldo filter in the arm-1 (solid line) and normalized axial PSF of the 2PE microscope with the Toraldo filter (dot dashed line). The values of wavelengths are: $\lambda_1 = 785.3$ nm, $\lambda_2 = 815.3$ nm and $\lambda_{2p} = 800$ nm.

with 2PE configuration, and we can see that the effect is very similar.

6. Conclusion

In this paper, we have studied the effect of Toraldo filters in a 2CE microscopy system. The numerical results show that this kind of filters is very useful in 2CE technique because allow an improvement in axial resolution by 22% and the suppression of sidelobes. Even though the introduction of Toraldo filters decreases the amount of two-color energies that is utilized for 2CE, and higher excitation energies are required, the use of pinhole and misalignment problems can be avoided.

Acknowledgements

This work was supported by the Plan Nacional I + D + I (Grant DPI2003-4698), Ministerio de Ciencia y Tecnología, Spain. We also acknowledge the financial support from the Generalitat Valenciana, Spain (Grant grupos03/227). J. Lancis gratefully acknowledges financial support from the Universitat Jaume I (Programa de semestres subàtics 03/04).

References

[1] J.B. Pawley, Handbook of biological confocal microscopy, Plenum Press, New York, 1995.
[2] W. Denk, J.H. Strickler, W. Webb, Science 248 (1990) 73.
[3] V. Daria, C. Blanca, O. Nakamura, S. Kawata, C. Saloma, Appl. Opt. 37 (1998) 7960.
[4] S. Hell, K. Bahlmann, M. Schrader, A. Soini, H. Malak, I. Gryczynski, J. Lakowicz, J. Biomed. Opt. 1 (1996) 71.
[5] C. Blanca, C. Saloma, Appl. Opt. 40 (2001) 2722.
[6] A.I. Whiting, A.F. Abouraddy, B.E.A. Saleh, M.C. Teich, J.T. Fourkas, Opt. Express 11 (2003) 1714.
[7] M. Martínez-Corral, C.R. Martínez-Cuenca, I. Escobar, G. Saavedra, Appl. Phys. Lett. 85 (2004) 4319.
[8] J.R. Lakowicz, I. Gryczynski, H. Malak, Z. Gryczynski, Photochem. Photobiol. 64 (1996) 632.
[9] I. Gryczynski, H. Malak, J.R. Lakowicz, Biospect. 3 (1997) 97.
[10] M. Cambaliza, C. Saloma, Opt. Commun. 184 (2000) 25.
[11] C.M. Blanca, C. Saloma, Appl. Opt. 70 (2001) 2722.
[12] M. Lim, C. Saloma, Opt. Commun. 207 (2002) 111.
[13] J.E.M. Goldsmith, Opt. Lett. 7 (1982) 437.
[14] J. Palero, W. Garcia, C. Saloma, Opt. Commun. 211 (2002) 57.
[15] M. Lim, C. Saloma, Appl. Opt. 42 (2003) 3398.
[16] S. Lindek, E.H.K. Stelzer, Opt. Lett. 24 (1999) 1505.
[17] F. Xiao, G. Wang, Z. Xu, Opt. Commun. 228 (2003) 225.

[18] J. Chen, K. Midorikawa, Opt. Lett. 29 (2004) 1354.
[19] M. Gu, Advanced optical imaging theory, Springer, Berlin, 2000, p. 143.
[20] B. Richards, E. Wolf, Proc. Roy. Soc. (London) A 253 (1959) 368.
[21] G. Toraldo di Francia, Atti Fond. Giorgio Ronchi 7 (1952) 366.
[22] D.M. de Juana, V.F. Canales, P.J. Valle, M.P. Cagigal, Opt. Commun. 229 (2004) 71.
[23] D.M. de Juana, J.E. Oti, V.F. Canales, M.P. Cagigal, J. Opt. Soc. Am. A 11 (2003) 2172.
[24] M. Martínez-Corral, M.T. Caballero, E.H.K. Stelzer, J. Swoger, Opt. Express 10 (2002) 98.
[25] E.H.K. Stelzer, S. Lindek, Opt. Commun. 111 (1994) 536.
[26] S. Lindek, J. Swoger, E.H.K. Stelzer, J. Mod. Opt. 46 (1999) 843.
[27] S. Hell, E.H.K. Stelzer, Opt. Commun. 93 (1992) 277.